JOURNAL OF COMPUTATIONAL PHYSICS 86, 440–465 (1990)

Two-Phase Flow in Porous Media with Multicomponent Transport: Formulation and Higher Order Numerical Solution

LAWRENCE J. ROBERTS AND KENNETH S. SORBIE*

Oil Recovery Projects Division, AEE Winfrith, Dorchester, Dorset, DT2 8DH, England

Received February 17, 1988; revised October 10, 1988

This paper presents a novel formulation of the two phase multicomponent transport equations including reaction and adsorption of the transported chemical components. The equations describing the phase saturation and the components transport within the phase are written and treated in a very similar way. The resulting set of coupled non-linear convection–dispersion equations is posed as an initial-boundary value problem which is conveniently formulated for numerical solution using an extended method of lines approach. The method of lines offers two main advantages for the solution of this system of equations when compared with lower order methods. The non-linear terms are treated in a straightforward manner and the spatial derivatives can be represented with greater accuracy to high order without undue complication. Highly accurate results are obtained for single and two phase problems for which analytical results are known. © 1990 Academic Press, Inc.

1. INTRODUCTION

The most important example of two-phase flow in porous media is undoubtedly in the simultaneous flow of oil and water in petroleum reservoirs during oil recovery processes. Water is frequently injected into the reservoir to displace the oil. This waterflooding process often leaves much oil behind due to poor fluid sweep efficiency [1]. In order to improve the efficiency of the oil displacement process a number of enhanced oil recovery (EOR) methods have been developed and applied [2]. Polymer flooding [2] is an EOR process in which a small amount of polymer is added to the injected water in order to increase the viscosity of the aqueous phase and hence improve the sweep efficiency. Another related process involves injecting both polymer and a suitable metal ion to form a crosslinked time setting gel within the porous medium [4, 5].

To describe two-phase flow mathematically on a macroscopic scale, equations have been proposed based on a combination of the mass conservation equations

* Now with Department of Petroleum Engineering, Heriot-Watt University, Edinburg EH14 4AS, Scotland.

0021-9991/90 $3.00

and Darcy's law [6]. When the phenomenon of capillary pressure [7] is included in the two-phase flow equations for incompressible fluids, a generalized non-linear convection–dispersion equation is obtained [8, 9] which is only analytically soluble for a very limited class of problems [9]. If capillary pressure is neglected, the governing equation becomes hyperbolic and the analytic solution to this equation is the familiar solution of Buckley and Leverett [10]. In order to describe EOR processes such as polymer flooding, the formulation must be extended to include the transport of the chemical components within the aqueous phase. These species may show dispersion, adsorb onto the rock matrix [11, 12], react with other species [13], chemically degrade [14], and change the phase viscosity and rheology [15]. All of this behaviour must be taken into account in the transport equations.

In this paper, we formulate a set of generalised coupled convection–dispersion equations to describe two-phase multicomponent transport for a system in which there is capillary pressure, chemical reaction, and component adsorption. The equations for each of the components in the aqueous phase and for the water saturation are treated in a very similar way although their boundary conditions are rather different. The governing equations yield an initial-boundary value problem which is particularly suitable for numerical solution using a variation of the method of lines (MOL) [16]. The spatial terms are discretised to give a coupled set of ordinary differential equations (ODEs), which are solved numerically using one of several available ODE library subroutines. This method has two important advantages when applied to these transport equations. First, it is straightforward to deal with the non-linear terms arising from the reaction, adsorption, and capillary pressure terms in the equations. If finite difference methods are applied in the usual manner by discretising to low order in time and formulating a matrix problem, then the resulting equations require an iterative solution technique such as the Newton–Raphson [17] which may involve a large amount of computational effort to achieve adequate convergence. The second advantage in using the MOL is that the spatial derivatives in the convection and dispersion terms can easily be evaluated to very high order with very little extra computational effort. These higher order representations are particularly important for the convective term which leads to dispersive numerical truncation errors [18, 19] when approximated to low spatial order. If higher order terms were used within a conventional finite difference formulation [18], then, in addition to the non-linearities, much more broadly banded matrices would result, which are more difficult and time consuming to solve.

The high order numerical scheme which is developed in this paper is applied to some examples of 1D single and the two-phase problems. The results of these calculations are compared with analytical results. An example of two-phase multicomponent transport is presented where two components mix to produce a viscous third species. This *in situ* improvement in the mobility ratio leads to the formation of an oil bank and the recovery of incremental reservoir oil.

2. Formulation of the Physical and Mathematical Problems

In this section, we present the mathematical formulation that we have used to model multicomponent transport in 1D two-phase systems.

2.1. *Convection–Dispersion Equations in Two-Phase Flow*

In two-phase one-dimensional flow, consideration of the conservation of mass across an infinitesimal volume, allowing for convection, dispersion, adsorption, chemical reaction, and inaccessible pore volume [20, 21] yields the following continuity equation for the transported component in the aqueous phase whose concentration is C_i:

$$S_w \frac{\partial C_i}{\partial t} + \frac{\rho_r(1-\phi)}{\phi_i \rho_w} \frac{\partial C_{si}}{\partial t} + \frac{(\phi_i - \phi)}{\phi_i} \frac{C_i}{\rho_w} \frac{\partial}{\partial t}(\rho_w S_w)$$
$$= \frac{1}{\rho_w} \frac{\partial}{\partial x}\left(\rho_w D_i \frac{\partial C_i}{\partial x}\right) - \frac{U_w}{\phi_i} \frac{\partial C_i}{\partial x} + S_w R_i(\mathbf{C}), \tag{1}$$

where S_w is the water saturation, ρ_w is the water density, U_w is the aqueous phase Darcy velocity, and D_i is the diffusion/dispersion coefficient for component i within the aqueous phase. The rock porosity ϕ may differ from the component effective porosities ϕ_i because of excluded volume or inaccessible pore volume effects such as those frequently observed for polymeric species [20–22]. The vector $\mathbf{C}$ represents all of the transported species and $R_i(\mathbf{C})$ represents the rate of change of the concentration of component i due to chemical reaction. In this work we assume that the aqueous phase density is independent of its chemical composition. The adsorption of each component is described by the isotherm $C_{si}(\mathbf{C})$. If the system is at chemical equilibrium during the flow then, for an NC component system, Eq. (1) becomes

$$S_w \frac{\partial C_i}{\partial t} + \alpha_i \sum_{j=1}^{NC} \left(\frac{\partial C_{si}}{\partial C_j}\right)\left(\frac{\partial C_j}{\partial t}\right) + \beta_i C_i \left(\frac{\partial S_w}{\partial t}\right) = G_i, \tag{2}$$

where

$$\alpha_i = \frac{\rho_r}{\rho_w} \frac{(1-\phi)}{\phi_i} \tag{3}$$

$$\beta_i = \frac{(\phi_i - \phi)}{\phi_i} \tag{4}$$

and

$$G_i = \frac{\partial}{\partial x}\left(D_i \frac{\partial C_i}{\partial x}\right) - V_{w_i}\left(\frac{\partial C_i}{\partial x}\right) + S_w R_i(\mathbf{C}). \tag{5}$$

The term V_{w_i} represents the superficial velocity of the transported component i which is given by

$$V_{w_i} = U_w/\phi_i. \tag{6}$$

The adsorption behaviour couples together the time derivatives of all components on which the isotherm depends.

2.2. *Additional Equation for the Water Saturation*

In the absence of capillary pressure, the fractional flow of water, f_w, in an oil–water system is given by the expression

$$f_w(\mathbf{C}, S_w) = \frac{k_{rw}(S_w)\,\mu_o}{k_{rw}(S_w)\,\mu_o + k_{ro}(S_w)\,\mu_w(\mathbf{C})}, \tag{7}$$

where k_{rw}, k_{ro} are the saturation-dependent relative permeabilities [6, 18] of water and oil, respectively, and μ_w and μ_o are the water and oil viscosities. In general, μ_w may be a function of any dissolved components that contribute to the viscosity.

The presence of capillary pressure complicates the fractional flow equation since the oil and water pressure gradients are not equal. The velocities of the aqueous and oleic phases, U_w and U_o, are given by the generalised Darcy law expressions as

$$U_w = -\frac{kk_{rw}}{\mu_w}\left(\frac{\partial P_w}{\partial x}\right) \tag{8}$$

$$U_o = -\frac{kk_{ro}}{\mu_o}\left(\frac{\partial P_o}{\partial x}\right), \tag{9}$$

where the pressures in the water and oil phases, P_w and P_o, are related through the saturation dependent capillary pressure function:

$$P_c(S_w) = P_o - P_w. \tag{10}$$

It can be shown from Eq. (7)–(10), that the fractional flow of water is

$$F_w(\mathbf{C}, S_w) = f_w(\mathbf{C}, S_w) + \frac{A\phi}{Q}\, g(\mathbf{C}, S_w)\left(\frac{\partial S_w}{\partial x}\right), \tag{11}$$

where the function $g(\mathbf{C}, S_w)$ takes the form

$$g(\mathbf{C}, S_w) = \frac{kk_{rw}(S_w)\,k_{ro}}{\phi[k_{rw}(S_w)\,\mu_o + k_{ro}(S_w)\,\mu_w(\mathbf{C})]}\left(\frac{dP_c}{dS_w}\right). \tag{12}$$

A is the core cross-sectional area and Q is the water injection rate.
Conservation of mass for the aqueous phase requires that

$$\frac{\partial F_w}{\partial x} + \frac{A\phi}{Q}\frac{\partial S_w}{\partial t} = 0, \tag{13}$$

giving

$$\frac{\partial}{\partial x}\left[g(\mathbf{C}, S_w)\frac{\partial S_w}{\partial x}\right] + \frac{Q}{A\phi}\left(\frac{\partial f_w}{\partial x}\right) + \left(\frac{\partial S_w}{\partial t}\right) = 0. \tag{14}$$

Finally, we note that, since $f_w = f_w(\mathbf{C}, S_w)$,

$$\frac{\partial f_w}{\partial x} = \left(\frac{\partial f_w}{\partial S_w}\right)\left(\frac{\partial S_w}{\partial x}\right) - \frac{k_{ro}}{(k_{rw}\mu_o + k_{ro}\mu_w)^2} \sum_{j=1}^{NC} \left(\frac{\partial \mu_w}{\partial C_j}\right)\left(\frac{\partial C_j}{\partial x}\right). \tag{15}$$

The resulting transport equation is

$$\frac{\partial}{\partial x}\left[- g(\mathbf{C}, S_w)\frac{\partial S_w}{\partial x}\right] - \frac{Q}{A\phi}\left(\frac{\partial f_w}{\partial S_w}\right)\left(\frac{\partial S_w}{\partial x}\right) + \frac{k_{ro}}{(k_{rw}\mu_o + k_{ro}\mu_w)^2} \sum_{j=1}^{NC} \left(\frac{\partial \mu_w}{\partial C_j}\right)\left(\frac{\partial C_j}{\partial x}\right) = \frac{\partial S_w}{\partial t}. \tag{16}$$

This equation must be solved in conjunction with Eq. (2), subject to suitable boundary conditions.

If we write Eq. (16) as

$$G_w = \partial S_w / \partial t, \tag{17}$$

we can write the full coupled set of equations in matrix form as

$$\begin{bmatrix} S_w + \alpha_1\left(\frac{\partial C_{s_1}}{\partial C_1}\right) & \alpha_1\left(\frac{\partial C_{s_1}}{\partial C_2}\right) \cdots \alpha_1\left(\frac{\partial C_{s_1}}{\partial C_{NC}}\right) & \beta_1 C_1 \\ \alpha_2\left(\frac{\partial C_{s_2}}{\partial C_1}\right) & S_w + \alpha_2\left(\frac{\partial C_{s_2}}{\partial C_2}\right) \cdots \alpha_2\left(\frac{\partial C_{s_2}}{\partial C_{NC}}\right) & \beta_2 C_2 \\ \vdots & \vdots & \vdots \\ \alpha_{NC}\left(\frac{\partial C_{s_{NC}}}{\partial C_1}\right) & \cdots\cdots\cdots S_w + \alpha_{NC}\left(\frac{\partial C_{s_{NC}}}{\partial C_{NC}}\right) & \beta_{NC} C_{NC} \\ 0 & 0 \quad 0 & 1 \end{bmatrix} \begin{bmatrix} \frac{\partial C_1}{\partial t} \\ \frac{\partial C_2}{\partial t} \\ \vdots \\ \frac{\partial C_{NC}}{\partial t} \\ \frac{\partial S_w}{\partial t} \end{bmatrix} = \begin{bmatrix} G_1 \\ G_2 \\ \vdots \\ G_{NC} \\ G_w \end{bmatrix}. \tag{18}$$

2.3. *Initial and Boundary Conditions*

The initial conditions for all cases studied in this work are

$$C_k(x, 0) = 0; \qquad x > 0 \tag{19a}$$

$$S_w(x, 0) = S_{wc}; \qquad x > 0 \tag{19b}$$

where S_{wc} is the connate water saturation at which the water relative permeability is zero [6, 18].

The simplest boundary conditions that can be applied for the transported components are for the semi-infinite case where

$$C_k(0, t) = C_{ok}; \qquad x = 0 \cdots \tag{20a}$$

$$C_k(x, t) \to 0; \qquad x \to \infty \cdots. \tag{20b}$$

Equation (20a) must be modified slightly when a pulse of material is injected. More sophisticated inlet boundary conditions may be defined in order to model particular experiments more closely. For example, Bischoff and Levenspiel [23] set up model boundary conditions to describe entrance and exit sections in a single phase system of finite length. If dispersion coefficients are small, however, Eq. (20) provides a good approximation to the actual boundary conditions.

The boundary condition for the water saturation equation is

$$F_w = 1; \qquad x = 0 \cdots \tag{21a}$$

$$F_w \to 0; \qquad x \to \infty \cdots. \tag{21b}$$

Initially, when $S_w = S_{wc}$ at $x = 0$ and $f_w = 0$ at $x = 0$; the fractional flow of water at the inlet boundary is entirely due to the effects of capillary pressure. Inlet boundary conditions for two-phase flow in the presence of capillary pressure have been written in a number of ways [8, 9] although it is fairly straightforward to show that these are all equivalent.

3. Numerical Solution of the Coupled Transport Equations

The coupled set of equations to be solved for the evolution of the water saturation and transported component concentration profiles was given in Section 2.3. In the absence of inaccessible/excluded pore volume effects [22] ($\beta_i = 0$ for all i), these equations can be expressed in the form

$$T(S_w, \mathbf{C})\,\dot{\mathbf{C}} = \mathbf{G}(S_w, \mathbf{C}) \tag{22}$$

$$\frac{\partial S_w}{\partial t} = G_w(S_w, \mathbf{C}), \tag{23}$$

where T is the submatrix of component terms given in Eq. (18). In all cases in this paper, the above equations apply.

One approach to solving transport problems in chemical flooding [18, 24] is to use a straightforward discretization to low order in space and time. In one dimension, for example, the resulting tridiagonal system of equations can give reasonable accuracy for linear problems. However, the complications of chemical reaction, coupled adsorption, and the effects of two-phase flow give a set of non-linear equations which would require iterative solution or the use of non-linear solution techniques [25]. In addition, there are serious difficulties if either the time or spatial derivatives of Eqs. (22) and (23) are discretised to high order. High-order spatial discretizations, for example, lead to broad banded matrices which are much more difficult to solve than the tridiagonal system. To avoid these problems we employ the familiar method of lines which has been reviewed and applied recently by Byrne and Hindmarsh [16]. In the MOL, a partial differential equation is expressed as a system of coupled, non-linear ordinary differential equations (ODEs). This system

can be solved using one of the many robust and well-developed ODE solution algorithms [16, 26].

3.1. *The Method of Lines (MOL)*

To rewrite Eq. (22) and (23) as a set of ODEs we pre-multiply Eq. (22) by the inverse of matrix T to give

$$\dot{\mathbf{C}} = T^{-1}(S_w, \mathbf{C})\, \mathbf{G}(S_w, \mathbf{C}) \tag{24a}$$

$$\dot{S}_w = G_w(S_w, \mathbf{C}) \tag{24b}$$

and discretise only the *spatial* part of the resulting equations at the NX mesh points where the solution is required. This procedure gives the set

$$\frac{dY_k}{dt} = F_k(Y_1, Y_2, ..., Y_{NEQ}), \tag{25}$$

where $NEQ = (NC+1)^* NX$ for an NC component system, transported in the aqueous phase.

3.2. *Boundary Conditions*

For the components transported in the aqueous phase, the boundary conditions of Eq. (20) are imposed by specifying

$$\left.\frac{dY_k}{dt}\right|_{\text{INLET}} = 0; \qquad Y_k|_{\text{INLET}} = Y_k^{(0)} \tag{26}$$

and

$$\left.\frac{dY_k}{dt}\right|_{\text{OUTLET}} = \Omega(\mathbf{Y}), \tag{27}$$

where $\Omega(\mathbf{Y})$ is the backward-difference operator at the outlet point. A similar outlet boundary condition is imposed for the water saturation equation to model the semi-infinite problem. Other boundary conditions could be used to give capillary end-effects in finite systems [8, 27].

The inlet boundary condition of Eq. (21a) is more difficult to impose. Because the condition constrains the fractional flow of water, rather than the water saturation itself, it is necessary to deduce the time-dependence of the water saturation at the boundary. The continuity equation (13) is not useful at the inlet boundary, since the spatial derivative of the fractional flow can only be expressed to first order. We have obtained our best numerical results by using the mass balance condition to determine the rate of change of saturation at the inlet boundary:

$$Q_{\text{IN}} - Q_{\text{OUT}} = A\phi \int_0^L \frac{\partial S_w}{\partial t} \cdot dx, \tag{28}$$

where Q_{IN} and Q_{OUT} refer to the total volumetric injection and production rates of water only.

Making use of the trapezium rule we obtain, for example,

$$\left.\frac{dS_w}{dt}\right|_{INLET} = 2\left[\frac{(Q_{IN}-Q_{OUT})}{A\phi\Delta x} - \sum_{j=2}^{NX-1}\frac{dS_{wj}}{dt}\right] - \left[\frac{dS_w}{dt}\right]_{OUTLET}. \tag{29}$$

3.3. *Solution Strategy*

The set of Eq. (18) has now been formulated as an initial value problem in $(NC+1)^* NX$ unknowns. The solution strategy is:

(i) At each time within the integration process, evaluate the matrix T and the right-hand sides $\mathbf{G}$ and G_w using Eqs. (5), (17), and (18). Calculation of the G_i in Eq. (5) requires the velocities V_{wi} which are expressed in terms of the fractional flow of water:

$$V_{wi} = \frac{QF_w}{A\phi_i}. \tag{30}$$

(ii) Invert the matrix T. This inversion is trivial if the adsorption of each component depends only on its own concentration.

(iii) Construct the derivatives $\dot{\mathbf{C}}$, $\dot{S}_w$ at each mesh point using Eqs. (24), (26), (27), and (29).

(iv) Return the derivatives to the numerical ODE integrator so that the solution at the next time step is evaluated.

3.4. *Treatment of the Right-Hand-side, G_w*

Equation (17) shows that the transport terms for the water saturation equation take a very similar form to those of the transported components given in Eq. (5). The capillary dependent term $[g(\mathbf{C}, S_w)]$ behaves like a non-linear diffusion coefficient which evolves with the solution. Expansion of Eq. (17) gives

$$G_w = -g(\mathbf{C}, S_w)\frac{\partial^2 S_w}{\partial x^2} - \left[\frac{Q}{A\phi}\frac{\partial f_w}{\partial S_w} + \frac{\partial g}{\partial S_w}(\mathbf{C}, S_w)\right]\left(\frac{\partial S_w}{\partial x}\right)$$

$$+ \frac{k_{ro}}{(k_{rw}\mu_o + k_{ro}\mu_w)^2}\sum_{j=1}^{NC}\left(\frac{\partial \mu_w}{\partial C_j}\right)\left(\frac{\partial C_j}{\partial x}\right). \tag{31}$$

This expansion allows the water saturation equation to be solved in the same way as the component transport equations. The velocity term is modified by the addition of the term in $\partial g/\partial S_w$. The terms in $\partial f_w/\partial S_w$ and $\partial \mu_w/\partial C_j$ are evaluated analytically from specified functions $f_w(\mathbf{C}, S_w)$ and $\mu_w(\mathbf{C})$. The terms in $\partial C_j/\partial x$ have already been calculated when evaluating the G_i.

3.5. *Higher Order Discretisation*

The spatial derivatives in Eqs. (5) and (17) can be very accurately evaluated using high order central differences. The maximum number of pairs of points that can be used is given by

$$m = \text{MIN}(\text{MORD}, i-1, NX-i) \tag{32}$$

for the ith point, where MORD is the maximum number of pairs to be used in the calculation and the order of the approximation is $2m$. A first-order backward difference must be applied at the effluent point for first derivatives. The form of the general central difference expression for first derivatives, assuming points are equispaced is as follows:

$$\left(\frac{\partial C}{\partial x}\right)_i^{(m)} = \frac{1}{M_m} \sum_{j=1}^{m} A_j^{(m)} \left(\frac{C_{i+j} - C_{i-j}}{2j\Delta x}\right) + O(\Delta x^{2m}), \tag{33}$$

where the quantities, $A_j^{(m)}$, are related by recurrence relationships involving the binomial coefficients which can be simplified to

$$M_m = \frac{(2m)!}{2(m!)^2} \tag{34}$$

$$A_1^{(m)} = M_m \frac{2m}{m+1} \tag{35}$$

and

$$A_j^{(m)} = \left(\frac{m-j+1}{m+j}\right) A_{j-1}. \tag{36}$$

The second derivatives associated with dispersive terms are given to successive orders by

$$\left(\frac{\partial^2 C}{\partial x^2}\right)_i^{(1)} = \left(\frac{C_{i+1} - 2C_i + C_{i-1}}{\Delta x^2}\right) + O(\Delta x^2) \tag{37}$$

$$\left(\frac{\partial^2 C}{\partial x^2}\right)_i^{(2)} = \left(\frac{16(C_{i+1} + C_{i-1}) - (C_{i+2} + C_{i-2}) - 30C_i}{12\Delta x^2}\right) + O(\Delta x^4) \tag{38}$$

$$\left(\frac{\partial^2 C}{\partial x^2}\right)_i^{(3)} = \left(\frac{270(C_{i+1} + C_{i-1}) - 27(C_{i+2} + C_{i-2}) + 2(C_{i+3} + C_{i-3}) - 490C_i}{180\Delta x^2}\right) + O(\Delta x^6). \tag{39}$$

It is much more common in the numerical simulation of fluid flow in oil reservoir systems to use first- or second-order discretisation of derivatives. Either single or

two point upstream methods [29] are usually applied to the convective terms. We will present calculations later in this paper using these approximations for comparative purposes. The single point upstream representation is defined straightforwardly as

$$\left(\frac{\partial C}{\partial x}\right)_i = \left(\frac{C_i - C_{i-1}}{\Delta x}\right) + O(\Delta x), \tag{40}$$

where the flow is in the direction of increasing i. This approximation is accurate to first order and it is stabilised by the large amount of numerical dispersion which it introduces [19]. The two point upstream calculation must be performed using overshoot/undershoot controls in the calculation of the first derivative as

$$\left(\frac{\partial C}{\partial x}\right)_i = \left(\frac{C_{i+1/2} - C_{i-1/2}}{\Delta x}\right) + O(\Delta x^2), \tag{41}$$

where the algorithm for the undershoot and overshoot tests is given sequentially as

$$C_{i+1/2} = C_i - \tfrac{1}{2}(C_{i-1} - C_i) \tag{42a}$$

$$C_{i+1/2} = \mathrm{MAX}\{C_{i+1/2}, \mathrm{MIN}\{C_i, C_{i+1}\}\} \tag{42b}$$

$$C_{i+1/2} = \mathrm{MIN}\{C_{i+1/2}, \mathrm{MAX}\{C_i, C_{i+1}\}\}. \tag{42c}$$

Analogous tests are applied to $C_{i-1/2}$.

4. Comparison of High Order Method of Lines With Analytical Solutions

4.1. *The Single Phase Convection Dispersion Problem*

For a step concentration input, C_o, in a semi-infinite system the one component single phase convection–dispersion equation with boundary conditions given by Eq. (20) has analytical solutions [30]. Ogata [31] has given a solution for the case of a linear irreversible reaction or adsorption. This equation is obtained from Eq. (1) by setting S_w to unity, C_{si} to zero, and R_i to $k_1 C$, where k_1 is the first-order rate constant which may be negative (degradation) or positive (growth). For this case the analytic concentration profile $C_A(x, t)$, is given by

$$C_A(x, t) = \frac{C_o}{2}\left\{\exp\left[\frac{(1-\beta')\,vx}{2D}\right]\mathrm{erfc}\left[\frac{x-\beta' vt}{2(Dt)^{1/2}}\right] + \exp\left[\frac{(1+\beta')\,vx}{2D}\right]\mathrm{erfc}\left[\frac{x+\beta' vt}{2(Dt)^{1/2}}\right]\right\}, \tag{43}$$

where the constant, β', is given by

$$\beta' = \left[1 + \frac{4Dk_1}{v^2}\right]^{1/2} \tag{44}$$

and v and D are the velocity and dispersion coefficient, respectively, and erfc is the complementary error function [32].

In solving problems of this type numerically, we refer to the mesh Peclet number, Pe_m, defined by

$$\mathrm{Pe}_m = \frac{v\Delta x}{D}. \tag{45}$$

In our MOL numerical solution, a Runge–Kutta–Merson [26] ODE integrator was used. The ODE algorithm used has a fourth-order time truncation error. The target solution error in all cases was sufficiently small to give converged solutions. Although the numerical code can operate up to arbitrarily high order, the maximum order for the convective terms in this and most subsequent calculations is tenth. In the problems studied in this paper, this order ensures adequate convergence in most cases. In most cases, the dispersive terms are expressed to sixth order.

Figure 1 compares high order numerical calculations with analytical results for two problems, one in which there is first-order growth of concentration and the other in which there is no reaction. These problems are expressed in dimensionless

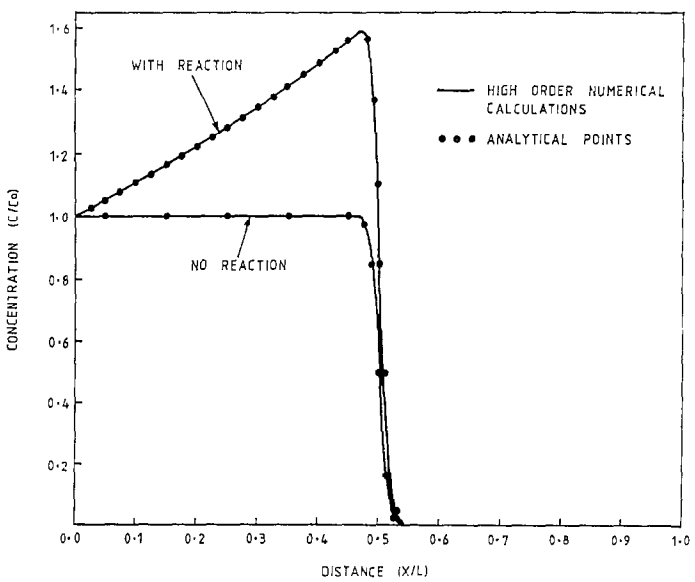

FIG. 1. Comparison of high order numerical calculations with analytic results for $\mathrm{Pe}_m = 40$.

form where $v = 1.0$, $D = 1.5625 \times 10^{-4}$, and $k_1 = 0$ and 1.0. For this case, $\Delta x = 6.25 \times 10^{-3}$ which corresponds to a mesh Peclet number of 40. Figure 2 compares the high order numerical calculation for one of these cases ($k_1 = 1.0$) with the MOL technique using single and two point upstream approximations. The single point calculation is stable but is very dispersed. The solution profile calculated using the two point upstream method appears to be a reasonably good fit to the analytical solution. However, the pointwise agreement is rather poor and artificial controls (see Eq. (42)) must be applied in order to remove spurious downstream overshoot [29].

Accurate agreement between the analytical and numerical concentration profiles may not be necessary in simple non-interacting systems for practical applications. However, in polymer cross-linker reacting systems where dispersive mixing may be necessary to initiate reaction, or in pressure constrained systems, high accuracy calculations are required for proper modelling of the system.

Analytical solutions for the constant velocity propagation of a pulse profile, again with linear adsorption/reaction terms, can be constructed from equation (43) using solution superposition. For a pulse input function of concentration C_o between time, $t = 0$, and $t = t'$ then the analytic profile, $C_B(x, t > t')$ is given by

$$C_B(x, t) = C_A(x, t) - C_A(x, t - t'). \tag{46}$$

Comparisons between the higher order, single-point upstream and second-order central difference calculations are shown for cases of pulse propagation in Figs. 3

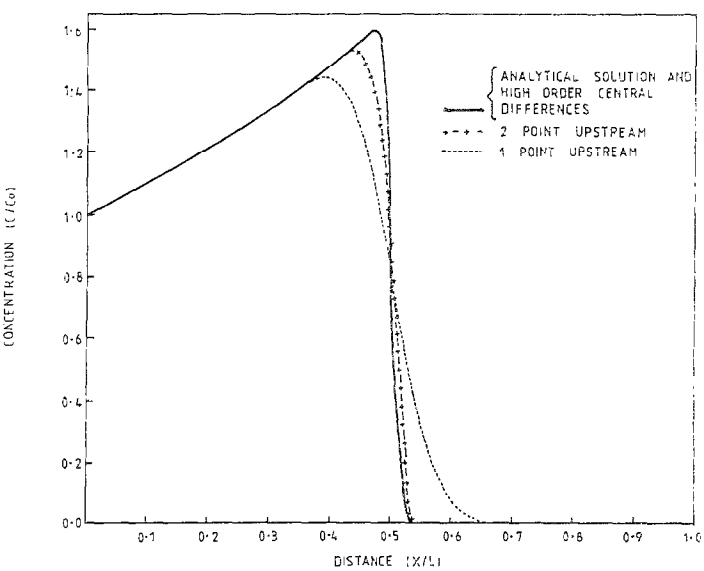

FIG. 2. Comparison of high order numerical calculation with single and two-point upstream approximation for $Pe_m = 40$.

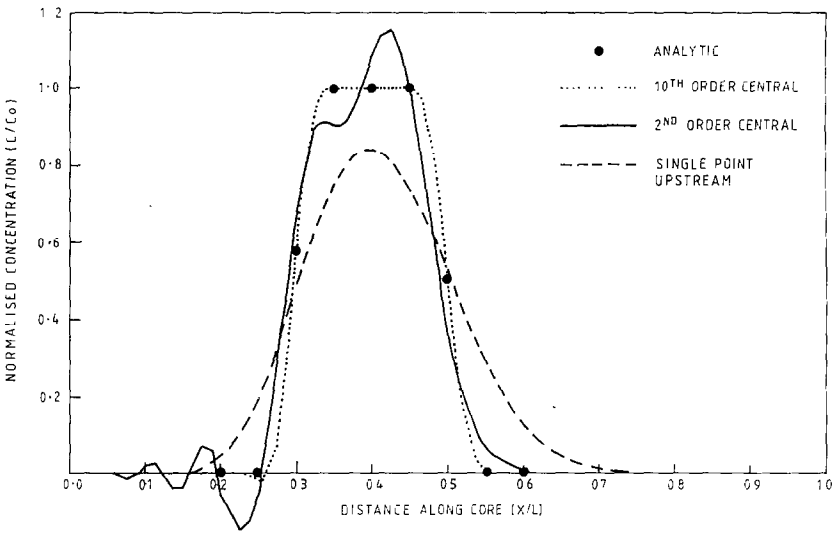

FIG. 3. Analytical and numerical concentration profiles for $Pe_m = 40$.

and 4. The system details are identical in these cases with $v = 3.5 \times 10^{-3}$ cms^{-1}, the difference being that the mesh Peclet number is 40 in Fig. 3 ($D = 1.1 \times 10^{-5}$ cm^{2}s^{-1}) and 20 ($D = 2.2 \times 10^{-5}$ cm^{2}s^{-1}) in Fig. 4. These figures illustrate not only the accuracy of the higher order scheme but its effect on the stability of the numerical solution to the (linear) convection–dispersion equation.

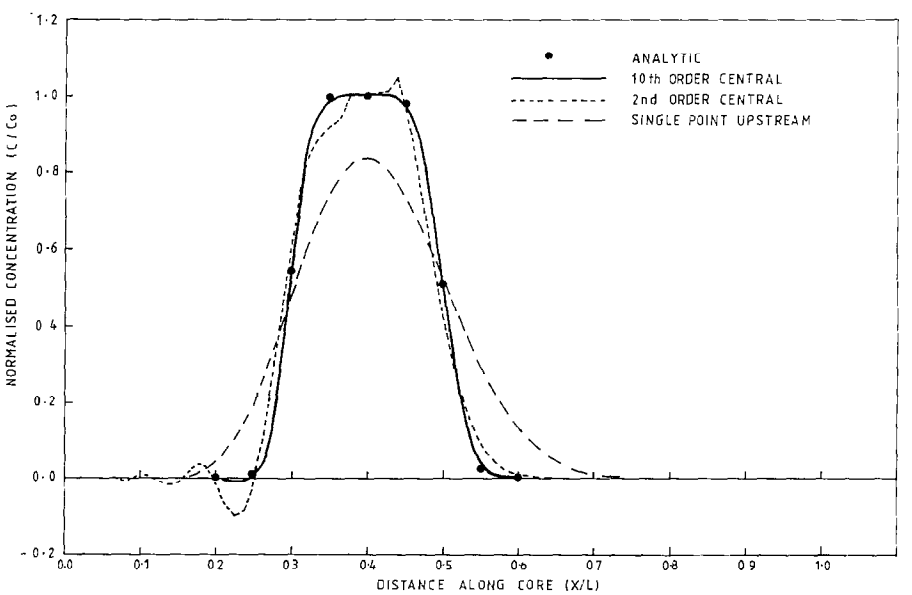

FIG. 4. Analytical and numerical concentration profiles for $Pe_m = 20$.

The second-order central difference solutions in both Fig. 3 and 4 show a con-

quantity must be less than 2 for stable non-oscillating central difference solutions to be obtained [34]. The 10th-order central difference scheme agrees almost exactly with the analytical solution on the scale of this figure. However, there is a very small amount of upstream undershoot on the higher order solution which is barely visible on the figure and poses no practical problems.

A more objective test of the pointwise convergence properties of the high-order, single point and two point schemes may be performed by defining average pointwise error, ε, as

$$\varepsilon = \frac{1}{NX} \sum_{i=1}^{NX} |C_{i_{\text{calc}}} - C_{i_{\text{analytic}}}|. \tag{47}$$

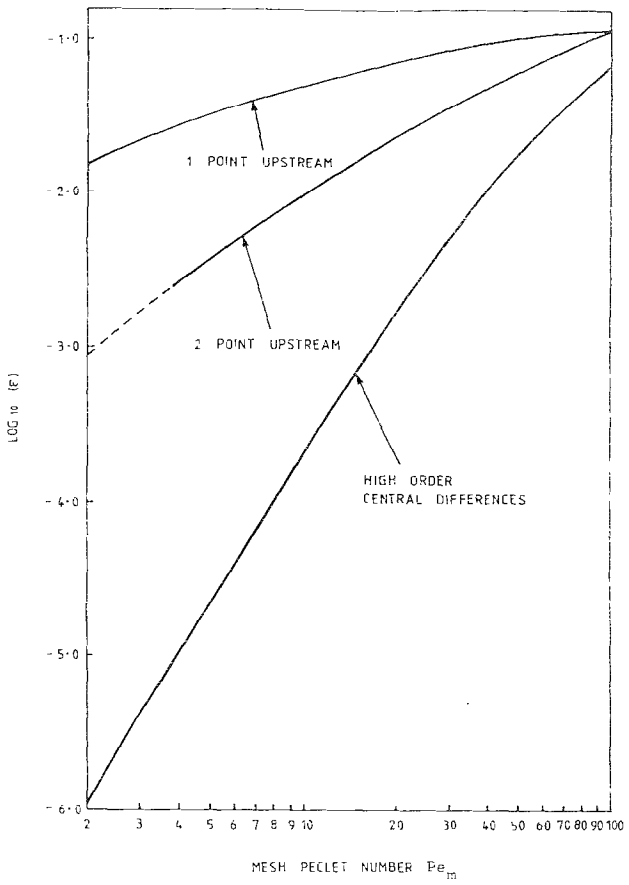

FIG. 5. Pointwise convergence of the high order, single and two-point upstream calculations vs mesh Peclet number.

The log of ε is plotted against the mesh Peclet number, Pe_m, for the lower and higher order schemes applied to the linear convection–diffusion equation in Fig. 5. It is seen that the convergence of the high order method is very much more rapid than that of the lower order schemes. For example, to achieve an average pointwise error of ~ 0.1 % the high order scheme can work at a mesh Peclet number of ~ 10; for the same accuracy the two-point upstream scheme must work at a mesh Peclet number of ~ 1 and the single point upstream scheme must have $\mathrm{Pe}_m \ll 1$. Thus the two-point upstream discretisation would require a spatial grid about ten times as fine as the high order scheme for the same accuracy. We note that the convergence of the higher order scheme does not, as might first be expected, become more rapid as we go to successively finer grids (lower mesh Peclet number). This can be seen from Fig. 5, where the overall convergence rate is only of order ~ 3.5. This is due to the effect of the lower order approximations close to the boundaries. The full benefit of a higher order scheme may only be obtained for the propagation of a profile from a region within the system away from the boundaries.

TABLE I

Data for the Model Cases

A	Cross-sectional area	$= 15.9\ \mathrm{cm}^2$
Q	Injection rate	$= 0.008333\ \mathrm{cm}^3/\mathrm{s}$
k	Absolute permeability	$= 0.349$ Darcy
ϕ	Porosity	$= 0.176$
L	Length of core[a]	$= 10$ cm

Relative permeability curves

$$k_{rw}(S_w) = S_w - S_{wc}$$

$$k_{ro}(S_w) = 1 - S_{or} - S_w$$

S_{wc}	Connate water saturation	$= 0.0375$
S_{or}	Residual oil saturation	$= 0.15$
μ_o	Oil viscosity	$= 2.18$ cp
M	Viscosity ratio	$= \mu_w/\mu_o$

	$M = 4;\ \beta = 10$[b]
Water viscosity, μ_w $(mPas)$	8.720
Characteristic capillary pressure gradient $\left(\frac{dP_c}{dS_w}\right)_{ch}$ (Pa)	33.172
constant γ/β	0.12083

[a] A finite core length is considered for convenience and presentation in these cases although the analytical solution is strictly for a semi-infinite system.

[b] See the work of Yortsos and Fokas [9, 33] for results relating to other values of parameters M and β.

4.2. *Analytical Solutions of the Two-Phase Problem with Capillary Pressure*

Analytical solutions to the two-phase flow problem in porous media in the presence of capillary pressure are only available for a limited class of problems [9, 33]. Although the solution is limited to linear relative permeability curves and a particular form of the capillary pressure function $P_c(S_w)$, the result provides a useful analytical check on the numerical method for the solution of the water saturation equation described in Section 3. In this section, we present a comparison of our numerical method with this analytical solution for a waterflood, where viscous forces dominate but where some effect of capillary pressure is evident. Only in such cases is the saturation front sufficiently sharp to require higher order methods. When capillary pressure is dominant the fronts are so spread out [9, 33] that low order methods are adequate.

The details of the waterflood are given in Table I. The relative permeability functions in Table I are linear. All other quantities are defined in the table except for the parameters γ and β. The ratio of these quantities is used in the analytical definition of the capillary pressure function, $P_c(S_w)$, as shown below. Only the derivative of capillary pressure is required in the analytic solution and Yortsos and Fokas [9] give an expression for this quantity. We have obtained the following form of the capillary pressure to within an additive constant by integrating their formula

$$P_c(S_w) = \frac{1}{\left(S_{or} + \frac{\gamma}{\beta}\right)} \left(\frac{dP_c}{dS_w}\right)_{ch} \left[\frac{1}{\left(S_{or} + \frac{\gamma}{\beta}\right)} \log_e \left(\frac{1 + \frac{\gamma}{\beta} - S_w}{1 - S_{or} - S_w} \right) \right.$$

$$\left. + \frac{1}{\left(1 + \frac{\gamma}{\beta} - S_{wc}\right)} \log_e \left(\frac{S_w - S_{wc}}{1 + \frac{\gamma}{\beta} - S_{wc}} \right) \right], \tag{48}$$

where $(dP_c/dS_w)_{ch}$ is the constant characteristic capillary pressure gradient given in Table I for the cases studied here. The integration constant is taken to be zero in Eq. (48) above. The case presented in this paper and other related calculations are discussed fully in Yortsos and Fokas [9, 33].

In applying our numerical method to the calculation of water saturation profiles with capillary pressure, it is inappropriate to quote a fixed mesh Peclet number since the dispersive term is the non-linear saturation dependent capillary pressure term which varies along the system. If a sufficiently fine grid is used for the calculation, 81 grid points in this case, then a reasonably good practical fit to the analytic solution is obtained for a second-order convective term as shown in Fig. 6. However, when this solution is examined more closely the very high pointwise accuracy of the higher order numerical scheme becomes clear. Table II compares the 81 grid point calculations using different orders of approximation to the convective term. The single point upstream approximation gives a very poor fit to the

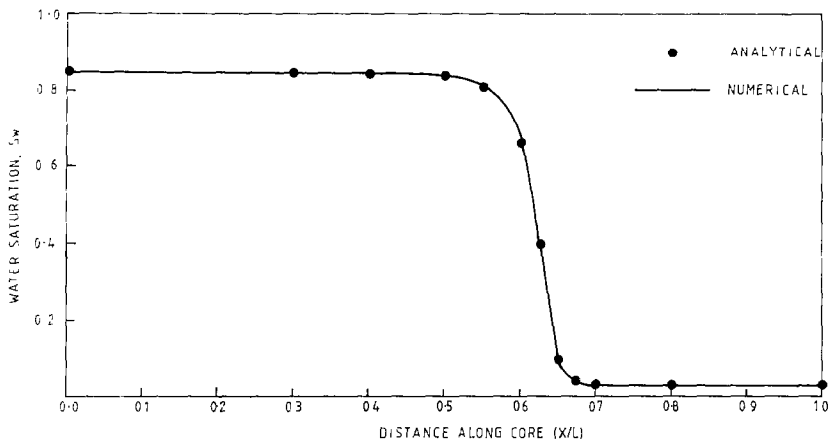

FIG. 6. Comparison of analytical and second-order numerical (81 mesh point) saturation profile (at $t = 1679$ s).

saturation profile. In the plateau region behind the water front ($S_w = 1 - S_{OR} = 0.8500$), the saturation value is calculated with a 2.5 % error for the single point approximation. This source of error is gradually removed as the order of the numerical solution is increased as shown in Table II. This effect is accentuated as the number of grid points is reduced. Figure 7 shows a comparison between a low (second-order convection and dispersive terms) and higher order (10th-order convective; 6th-order dispersive term) calculation of case A with only 21 mesh points. The higher order calculation is more accurate both behind the saturation front and in the region of this front. This is due to the inlet boundary condition (Eq. (29)) which imposes mass conservation. Errors in the phase velocity at the flood front

TABLE II

Numerical Solution for the Two-Phase Displacement for Different Convective Orders (Dispersive Order = 6; $NX = 81$)

x (cm)	Analytical	1 pt. upstream	2nd order	4th order	6th order	10th order
0.0	0.8500	0.8712	0.8482	0.8497	0.8499	0.8500
3.0	0.8500	0.8710	0.8482	0.8497	0.8499	0.8500
4.0	0.8494	0.8689	0.8477	0.8491	0.8493	0.8494
5.0	0.8409	0.8456	0.8404	0.8406	0.8408	0.8409
5.5	0.8123	0.7803	0.8151	0.8122	0.8123	0.8124
6.0	0.6644	0.5232	0.6741	0.6662	0.6647	0.6643
6.25	0.4014	0.2671	0.4051	0.4037	0.4023	0.4018
6.5	0.1033	0.0921	0.1116	0.1054	0.1039	0.1034
6.75	0.0425	0.0460	0.0447	0.0425	0.0425	0.0425
7.0	0.0378	0.0387	0.0381	0.0378	0.0378	0.0378
8.0	0.0375	0.0375	0.0375	0.0375	0.0375	0.0375

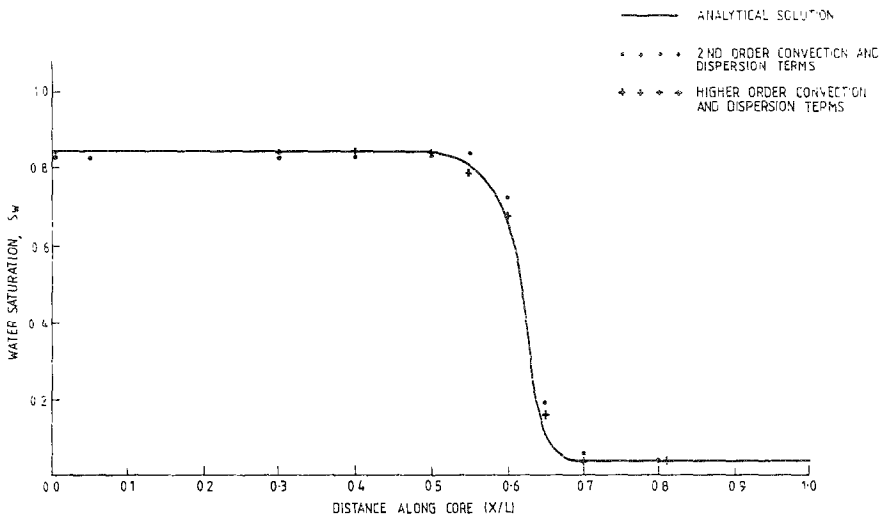

FIG. 7. Comparison of 2nd and high order discretisation for saturation profile in two-phase flow.

due to numerical inaccuracies, have a feedback effect on the boundary condition and hence affect the plateau height. Although the dispersive term in Table II is also calculated to higher (sixth) order, it is shown in Table III that this does not have a very important effect on the accuracy of the case A numerical solutions.

For the high order scheme, the effect of mesh refinement is illustrated in Table IV. A comparison of the second-order results in Table II with the higher order results in Table IV, indicates that the higher order scheme does rather better than the lower order in terms of pointwise accuracy, with half the number of mesh points.

TABLE III

Numerical Solution for the Two-Phase Displacement for Different Dispersive Orders (Convective Order = 10th)

x (cm)	Analytical	2nd order	4th order	6th order
0.0	0.8500	0.8497	0.8500	0.8500
3.0	0.8500	0.8497	0.8500	0.8500
4.0	0.8494	0.8491	0.8494	0.8494
5.0	0.8409	0.8402	0.8409	0.8409
5.5	0.8123	0.8109	0.8123	0.8124
6.0	0.6644	0.6650	0.6639	0.6643
6.25	0.4014	0.4018	0.4023	0.4018
6.5	0.1033	0 1041	0.1034	0.1034
6.75	0.0425	0.0440	0.0426	0.0425
7.0	0.0378	0.0381	0.0378	0.0378
8.0	0.0375	0.0375	0.0375	0.0375

TABLE IV

Numerical Solution for the Two-Phase Displacement for Different Mesh Sizes (Convective Order = 10th; Dispersive Order = 6th)

x/L	Analytic	$NX = 21$	$NX = 41$	$NX = 81$	$NX = 161$
0.0	0.8500	0.8463	0.8497	0.8500	0.8500
3.0	0.8500	0.8460	0.8497	0.8500	0.8500
4.0	0.8494	0.8459	0.8492	0.8494	0.8494
5.0	0.8409	0.8410	0.8407	0.8409	0.8409
5.5	0.8123	0.7902	0.8126	0.8124	0.8124
6.0	0.6644	0.6834	0.6660	0.6643	0.6644
6.25	0.4014	—	0.4007	0.4018	0.4013
6.5	0.1033	0.1612	0.1098	0.1034	0.1032
6.75	0.0425	—	0.0415	0.0425	0.0425
7.0	0.0378	0.0320	0.0378	0.0378	0.0378
8.0	0.0375	0.0379	0.0375	0.0375	0.0375

5. An Example of Two-Phase Multicomponent Transport

In this section we illustrate the numerical solution procedure described in Section 3 for the two-phase multicomponent transport of a chemically reacting and adsorbing system. The product of the chemical reaction increases the viscosity of the drive water. The problem is based on the waterflood of Section 4 but uses a water viscosity of 0.545 cp. This gives a water/oil viscosity ratio of 0.25 and a correspondingly poor waterflood displacement efficiency. No analytical result is available for this case.

The generation of a viscous component in situ will lead to a local improvement in the mobility ratio and cause the formation of an oil bank. This is a similar situation to that proposed for the in situ gelation of polymers [35]. However, flow is in this case one dimensional and oil recovery is increased by improved microscopic (linear) sweep efficiency rather than by fluid diversion and crossflow as occurs in in situ gelation in stratified systems [35, 36]. We consider a three component system in which component A is injected as a pulse into the core during the initial waterflood. This component adsorbs strongly onto the reservoir rock and is consequently retarded. A second pulse of a different non-adsorbing component, B, is injected some time later which ultimately "catches" component A and a chemical reaction takes place in the region of dispersive mixing of A and B to produce a third component C (i.e., $A + B \rightarrow C$). The reaction rate is described by the second-order rate law

$$-\frac{1}{2}\frac{d[A]}{dt} = -\frac{1}{2}\frac{d[B]}{dt} = \frac{d[C]}{dt} = k_2[A][B], \tag{49}$$

where k_2 is the second-order (mass) rate law and the factor of $\frac{1}{2}$ ensures mass

conservation. We assume that component A adsorbs according to a linear isotherm such that

$$\frac{dC_{SA}}{dC_A} = \text{const.} \tag{50}$$

Component C contributes to the viscosity of the water through the linear relationship,

$$\mu_w([C]) = \mu_w([C]=0) + \xi[C], \tag{51}$$

where ξ is a constant.

Details of the parameters used in the calculation are given in Table V.

Figure 8 shows the predicted normalised concentration profiles of components A, B, and C at $t = 4000$ s. Component C can be seen at the intersection of the component A and component B profiles where chemical reaction has occurred. Figure 9 shows the water saturation profile that has developed as a result of the in situ chemical reaction. The profile for the no reaction ($k_2 = 0$) case has been drawn for comparison. The oil bank generated by the formation of component C can be seen

TABLE V

Parameters Used in Multicomponent Transport Example

μ_w	Water viscosity	$= 0.545$ cp
ξ	Coefficient of viscosity for component C	$= 1.0$ cp
M	Mobility ratio	$= 0.25$
	Characteristic capillary pressure gradient[a]	$= 3.2738 \times 10^{-4}$ atm
	Constant γ/β[a]	$= -1.2333$

Injection profile

Time (s)	Component + water
0–800	A
800–2400	—
2400–3200	B
3200–	—

Dispersion coefficient for all components	$= 2.0 \times 10^{-4}$ cm^2/s
Component porosities, ϕ_i = Rock porosity	$= 0.176$
Gradient of adsorption isotherm for component A	$= 0.1$
Density ratio ρ_{rock}/ρ_w	$= 2.6$
Chemical reaction rate k_2	$= 0.2$ s^{-1}

[a] See the work of Yortsos and Fokas [9, 33].

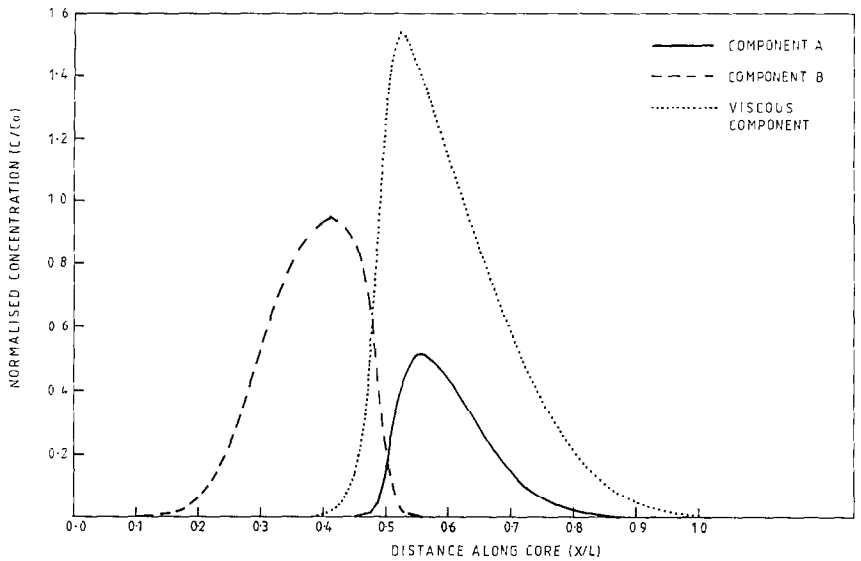

FIG. 8. Normalised component concentrations for multicomponent example $t = 4000$ s.

clearly. The resulting improvement in the profile of cumulative produced oil with time for the "gel" flood is compared with that of the base case waterflood in Fig. 10.

The example presented above was performed using higher order discretisation of the spatial terms with $NX = 81$ grid points as it was difficult to obtain a fully converged solution using a low order approximation. This calculation gives an

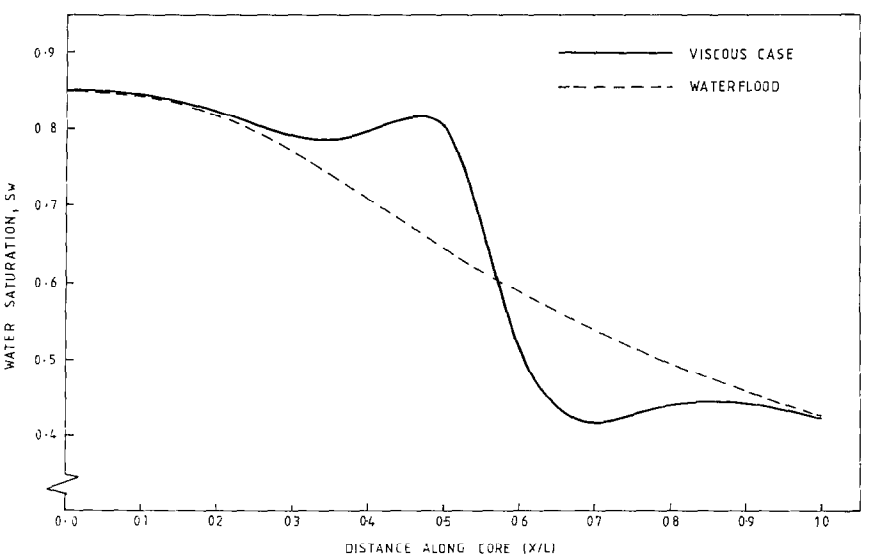

FIG. 9. Comparison of calculated water saturation profiles ($t = 4000$ s) for waterflood and viscous gel flood.

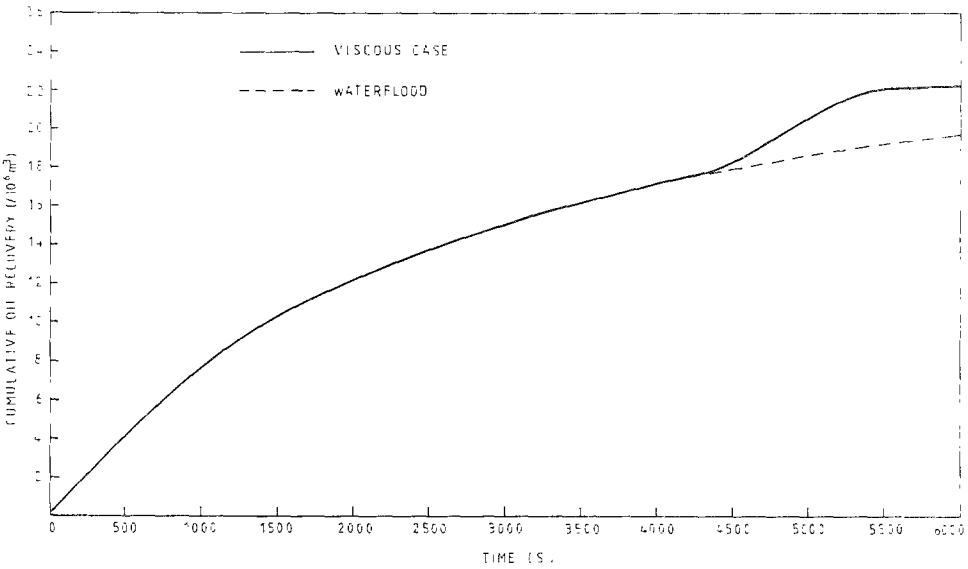

FIG. 10. Cumulative oil recovery for viscous case and waterflood.

illustration of the use of the high-order MOL method for more realistic non-linear two-phase multicomponent transport problems for which no analytical solution is known.

6. SUMMARY AND CONCLUSIONS

In this paper, we have formulated the general two-phase (oil/water) multicomponent transport equations in a novel way and have developed an accurate numerical method for their solution. The formulation unifies the treatment of the components transported in the aqueous phase and the water saturation evolution equation. Component dispersion, adsorption, chemical reaction, and inaccessible/excluded volume terms are incorporated into the coupled transport equations. A generalisation of the water saturation equation is derived which includes capillary pressure terms and the effect of viscous feedback on the local fractional flow. The equations for both the component and aqueous phase transport are similar in structure and together they form a coupled set of non-linear convection–dispersion equations. This set of equations is expressed in matrix form as an initial/boundary value problem with coupling between the component and saturation solutions. A simple Dirichlet boundary condition is adequate for transported components, whereas a more complex boundary condition applies for the phase saturation in the presence of capillary pressure.

The formulation described above is very conveniently posed for numerical solution using the method of lines (MOL). The two particular advantages of this

numerical solution technique are that the non-linear terms are dealt with very conveniently without using an iterative method and that it is very straightforward to extend the discretization of the spatial terms to higher order.

Comparison with both single and two-phase analytical results shows that using the higher order MOL gives excellent pointwise accuracy compared to low order finite difference methods. An example of multicomponent two-phase transport with chemical reaction and adsorption is presented for illustrative purposes only since no analytical solution exists for this problem.

The specific conclusions of this work are as follows:

(i) A novel general formulation of the two-phase multicomponent transport equations in porous media has been derived.

(ii) This formulation is very conveniently posed for numerical solution as an initial/boundary value problem.

(iii) A high-order method of lines solution has been developed which shows high pointwise accuracy for both single and two phase analytic solutions when compared with lower order methods on a given grid. It also handles non-linearities in the equations in a very convenient way.

(iv) The higher order scheme appears to stabilise oscillations for cases where the mesh Peclet number is >2.

(v) The convergence properties of the higher order scheme are affected by the lower order approximations at the boundaries.

(vi) For the water saturation equation, a mass balance boundary condition provides a convenient method of obtaining the correct saturation development at the boundary and along the entire system.

APPENDIX: NOTATION

A	Cross-sectional area of core
$A_j^{(m)}$	Coefficients in higher order discretization expression (33)
C_A, C_B, C_i	Concentrations of components A, B, and i
C_o	Concentration at inlet boundary (Dirichlet condition)
C_{ok}	Concentration at inlet boundary of component k
C_{si}	Concentration of adsorbed component i
$\mathbf{C}$	Vector of transport component concentration; $\dot{\mathbf{C}}$ time rate of change of $\mathbf{C}$
D	Dispersion coefficient
D_i	Dispersion coefficient of component i
f_w	Fractional flow of water without capillary pressure
F_k	Derivative function for the evolution of equation k
F_w	Fractional flow of water with capillary pressure
$g(S_w, \mathbf{C})$	Non-linear capillary dispersive term

G_i	Component i transport and reaction terms (Eq. (5))
G_w	Transport term of water
k	Absolute permeability
k_{ro}	Relative permeability to oil
k_{rw}	Relative permeability to water
k_1	First-order rate constant
k_2	Second-order rate constant
L	Length of core
M	Mobility ratio
M_m	Constant in expression for first derivatives using m nearest pairs
NC	Number of transported components in aqueous phase
NX	Number of mesh points
P_c	Capillary pressure
Pe_m	Mesh Peclet Number
P_o	Oil phase pressure
P_w	Water phase pressure
Q	Total volumetric injection rate of water
Q_{IN}	Volumetric injection rate of water
Q_{OUT}	Volumetric production rate of water
R_i	Chemical reaction rate of component i
S_{or}	Residual oil saturation
S_w	Water saturation
S_{wc}	Connate water saturation
t	Time
t'	Duration of pulse injection
$T(S_w, \mathbf{C})$	Matrix in Eq. (22)
U_w, U_o	Aqueous and oleic phase Darcy velocities
v	Superficial velocity; V_o oil velocity; V_w water velocity
V_{wi}	Superficial velocity of component i transported in the aqueous phase
x	Spatial co-ordinate
Y_k	kth solution to the coupled transport problem
$Y_k^{(o)}$	Boundary solution for the coupled transport problem
$\mathbf{Y}$	Vector of solutions evolved by ODE integrator
α_i	Adsorption density term as defined in Eq. (3)
β	Constant in Yortsos and Focas capillary pressure function
β'	Coefficient in Ogata expression
β_i	Inaccessible pore volume term for ith component (Eq. (4))
γ	Constant in Yortsos and Focas capillary pressure function
Δx	Mesh spacing
ε	Average pointwise absolute error
μ_o	Oil viscosity
μ_w	Water viscosity
ζ	Linear viscosity coefficient
ρ_r	Rock density

ρ_w	Water density
ϕ	Porosity
ϕ_i	Effective porosity to component i
$\Omega(\mathbf{Y})$	Outlet point backward difference operator
$\left(\frac{dP_c}{dS_w}\right)_{ch}$	Characteristic capillary pressure gradient
$\left(\frac{\partial C}{\partial x}\right)_i^{(m)}$	Approximation to the derivative at point i using m pairs of nearest points.

REFERENCES

1. F. F. CRAIG, *The Reservoir Engineering Aspects of Waterflooding* (SPE of AIME, New York, 1971).
2. H. K. VAN POOLEN, *Fundamentals of EOR* (Penwell, Tulsa, OK, 1980), Chap. 5.
3. H. L. CHANG, *J. Pet. Technol.* **1113**, August (1978).
4. J. P. BATYCKY, B. B. MAINI, AND G. MILOSZ, "A Study of the Application of Polymeric Gels in Porous Media," SPE 10620, Sixth International Symposium on Oilfield and Geothermal Chemistry, Dallas, TX, January 1982.
5. C. HUANG, D. W. GREEN, AND G. P. WILLHITE, "An Experimental Study of the In-Situ Gelation of Chromium^{+3}-Polyacrylamide Polymer in Porous Media," SPE/DOE 12638, Fourth SPE/DOE, Symposium on Enhanced Oil Recovery, Tulsa, OK, April 15–18, 1984.
6. R. E. COLLINS, *Flow of Fluids Through Porous Materials*, (Reinhold, New York, 1961).
7. M. MUSKAT, *Physical Principles of Oil Production* (McGraw–Hill, New York, 1949).
8. J. DOUGLAS, P. M. BLAIR, AND R. J. WAGNER, *Pet. Trans. AIME* **213**, 96 (1958).
9. Y. C. YORTSOS AND A. S. FOKAS, "An Analytical Solution for Linear Waterflood Including the Effects of Capillary Pressure," SPE 9407, 55th Annual Fall Conference of SPE, Dallas, TX, September 21–24, 1980.
10. S. E. BUCKLEY AND M. C. LEVERETT, *Trans. AIME* **146**, 107 (1942).
11. N. MUNGAN, *J. Canad. Pet. Technol.* **8**, 45 (1969).
12. G. J. HIRASAKI AND G. A. POPE, *Soc. Pet. Eng. J.* **337**, August (1974).
13. S. HUBBARD, L. J. ROBERTS, AND K. S. SORBIE, "Experimental and Theoretical Investigation of Time-Setting Polymer Gels in Porous Media," Fifth SPE/DOE Symposium on Enhanced Oil Recovery, Tulsa, OK, April 20–23, 1986.
14. P. J. CLIFFORD AND K. S. SORBIE, "The Effects of Chemical Degradation on Polymer Flooding," SPE 13586, International Symposium on Oilfield and Geothermal Chemistry, Phoenix, AZ, April 9–11, 1985.
15. R. K. PRUD'HOMME, J. T. UHL, J. P. POINSATTE, AND F. HALVERSON, *Soc. Pet. Eng. J.* **804**, October (1983).
16. G. D. BYRNE AND A. C. HINDMARSH, *J. Comput. Phys.* **70**, 1 (1987).
17. C. F. GERALD, *Applied Numerical Analysis*, 2nd ed. (Addison-Wesley, Reading, MA, 1980).
18. D. W. PEACEMAN, *Fundamentals of Numerical Reservoir Simulation* (Elsevier, New York, 1977).
19. R. B. LANTZ, *Soc. Pet. Eng. J.* **11**, 315 (1971).
20. R. DAWSON AND R. B. LANTZ, *Soc. Pet. Eng. J.* **448**, October (1972).
21. G. CHAUVETEAU, *J. Rheol.* (NY) **26**, 111 (1982).
22. W. C. LIAUH, J. L. DUDA, AND E. E. KLAUS, *AIChE Symposium Series 212* **78**, 70 (1982).
23. K. B. BISCHOFF AND O. LEVENSPIEL, *Chem. Eng. Sci.* **17**, 245 (1962).
24. P. L. BONDOR, G. J. HIRASAKI, AND M. J. THAM, *Soc. Pet. Eng. J.* **369**, October (1972).
25. M. AVRIEL, "*Nonlinear Programming; Analysis and Methods*," (Prentice–Hall, Englewood Cliffs, NJ, 1976).

26. W. F. AMES, *Numerical Methods for Partial Differential Equations*, 2nd ed. (Academic Press, New York/London, 1977).
27. F. M. PERKINS, *Trans. AIME* **210**, 409 (1957).
28. K. S. SORBIE, L. J. ROBERTS, AND R. W. S. FOULSER, "Polymer Flooding Calculations for Highly Stratified Brent Sands in the North Sea," Second European Symposium on Enhanced Oil Recovery, Paris, November 8–10, 1982.
29. M. R. TODD, P. M. O'DELL, AND G. J. HIRASAKI, *Soc. Pet. Eng. J.* **515**, December 1972.
30. M. T. VAN GENUCHTEN AND W. J. ALVES, U.S. Dept. of Agriculture, Technical Bulletin No. 1661, June 1982 (unpublished).
31. A. OGATA, Thesis, Northwestern University, Evanston, IL, 158 (unpublished).
32. M. R. SPEIGEL, *Mathematical Handbook of Formulas and Tables*, (McGraw-Hill, New York, 1968).
33. A. S. FOKAS AND Y. C. YORTSOS, *SIAM J. Appl Math.* **42**, 2 (1982).
34. H. S. PRICE, R. S. VARGA, AND J. R. WARREN, *Math. Phys.* **45**, 301 (1966).
35. T. SCOTT, L. J. ROBERTS, S. R. SHARPE, P. J. CLIFFORD, AND K. S. SORBIE, "In Situ Gel Calculations in Complex Reservoir Systems Using a New Chemical Flood Simulator," SPE 14234, 60th Annual Fall Conference of SPE, Las Vegas, September 22–25, 1985.
36. M. K. ABDO, H. S. CHUNG, C. H. PHELPS, AND T. M. KLARIC, "Field Experience with Floodwater Diversion by Complexed Biopolymers," Fourth SPE/DOE Symposium on Enhanced Oil Recovery, Tulsa, OK, April 16–18, 1984.